Nuclear Engineering and Technology 55 (2023) 1045–1051

Contents lists available at ScienceDirect

Nuclear Engineering and Technology

journal homepage: www.elsevier.com/locate/net

Original Article

Flexible liquid light-guide-based radiation sensor with $LaBr_3$:Ce scintillator for remote gamma-ray spectroscopy

Jae Hyung Park, Siwon Song, Seunghyeon Kim, Taeseob Lim, Jinhong Kim, Bongsoo Lee*

School of Energy Systems Engineering, Chung-Ang University, Seoul, 06974, South Korea

ARTICLE INFO

Article history:
Received 30 August 2022
Received in revised form
28 October 2022
Accepted 16 November 2022
Available online 17 November 2022

Keywords:
Liquid light guide
$LaBr_3$:Ce scintillator
Gamma-ray spectroscopy
Remote sensing
Energy resolution

ABSTRACT

In this study, we fabricated a liquid light-guide-based radiation sensor with a $LaBr_3$:Ce scintillator for remote gamma-ray spectroscopy. We acquired the energy spectra of Cs-137 and Co-60 using the proposed sensor, estimated the energy resolutions of the full energy peaks, and compared the scintillation light output variations. The major peaks of the radionuclides were observed in each result, and the estimated energy resolutions were similar to that of a general NaI(Tl) scintillation detector without a liquid light guide. Moreover, we showed the relationships of energy resolution and analog-to-digital channel regarding the number of photoelectrons produced and confirmed the effects of light guide length on remote gamma-ray spectroscopy. The proposed sensor is expected to be utilized to perform remote gamma-ray spectroscopy for distances of 3 m or more and would find application in many fields of nuclear facilities and industry.

1. Introduction

With an increase in the generation and use of radioactive isotopes in various fields such as medical, industry, and nuclear facilities, the risk of exposure to radioactive residues has increased. For public safety, continuous monitoring and accurate measurement of radiological contamination are required [1]. As part of radiation monitoring, quantitative measurements of radioactivity or dose are generally conducted; however, radionuclide identification that reveals the causal materials of contamination is more essential. Through radionuclide identification, specifying the cause of contamination, preventing additional risk with appropriate actions, and promoting public safety is possible.

Gamma-ray spectroscopy, which is an appropriate method for identifying and quantifying radionuclides, is widely utilized in radiological leakage monitoring of nuclear facilities, assay of radioactive wastes, and decontamination evaluation of post-processing such as decommissioning and remediation. For example, during post-processing, gamma-ray spectroscopy should be conducted to verify the radionuclides and their radioactivity levels at the site before and after the work, and decision should be taken to recycle or dispose the generated radioactive wastes [2,3].

For accurate evaluation of gamma-ray-emitting radionuclides, the measurement should be performed near the region of interest on site, or a sample analysis should be performed in the laboratory. However, in some cases, the region is inaccessible owing to the safety-critical nature of nuclear facilities, and workers could be exposed to excessive radiation. In addition, in the case of subjects that may be contaminated inside, such as pipe structures generated during decommissioning, radiation survey is usually conducted only on their exterior, thereby limiting the effectiveness of measurements [4,5]. Thus, there is a need to develop a radiation measurement system that is available in narrow spaces and can sense remotely with excellent performance.

Several studies on developing optical fiber-based radiation sensors for remote gamma-ray spectroscopy have been conducted in recent years. For example, Han et al. proposed a fiber-optic radiation sensor (FORS) comprising LYSO:Ce and plastic optical fiber (POF) [6]. They compared the scintillating light output of three different inorganic scintillators (BGO, YSO:Ce, and LYSO:Ce) irradiated by gamma-ray sources (Cs-137, Na-22, and Co-60) and measured their gamma-ray energy spectra. Yoo et al. measured the gamma-ray energy spectra and discriminated species of radioactive isotopes in a mixed radiation field using a FORS [7]. Further, Song et al. showed the variation in gamma-ray energy spectrum of Cs-137 with different lengths of a FORS and estimated the energy resolution [8]. As a long-distance light guide and remote-sensing tool, a POF has many advantages such as high flexibility, good processability, and electromagnetic interference immunity [6–9]. However, because of its small diameter, a large scintillator cannot

* Corresponding author.
E-mail address: bslee@cau.ac.kr (B. Lee).

https://doi.org/10.1016/j.net.2022.11.011

be used, and usually significant light loss occurs along the POF. Furthermore, its light transmissivity is limited in a certain wavelength region such as ultraviolet (UV), and it could be damaged in a high-level radiation field [10,11].

A liquid light guide (LLG), unlike a typical optical fiber, has a liquid-state material in the core. It has good light transmissivity in broad wavelength regions and can be manufactured with a larger diameter than the optical fiber. Additionally, it can deliver light with much greater intensity and low attenuation along the length because there is no packing fraction and it has very high radiation-resistant characteristics [11,12]. In particular, because of its good transmissivity in the UV–visible wavelength region, the LLG can be used as a light guide with various types of scintillators for radiation sensing, thereby enabling the development of remote radiation sensors with better energy resolution.

Recently, lanthanide scintillators such as $LaBr_3$:Ce and $CeBr_3$ have been in the spotlight as the optimum choice for gamma-ray detection in various fields owing to their excellent properties [13–16]. Nevertheless, because of the mismatching between the emission wavelength of the scintillators and the transmission wavelength of an optical fiber, lanthanide scintillators cannot be used in a FORS system. In previous FORS studies [6–8], different kinds of inorganic scintillators were used, which have much higher emission wavelengths than lanthanide scintillators and matched the transmission ranges of an optical fiber, for remote gamma-ray spectroscopy. However, with the LLG, the scintillation light from the lanthanide scintillators could be transferred well with a long attenuation length and low interfacial loss, and a larger scintillator could be used for high detection efficiency compared with the FORS system.

In this study, we developed an LLG-based radiation sensor system for remote gamma-ray spectroscopy. We fabricated a radiation sensor using a lanthanide scintillator and LLG and acquired energy spectra of Cs-137 and Co-60 remotely. Furthermore, the results of gamma-ray spectroscopy using different lengths of LLG were compared with those obtained without LLG. In addition, the variations in energy resolution and scintillation light output were estimated.

2. Materials and methods

A $LaBr_3$:Ce scintillator ($LaBr_3$:Ce, Epic Crystal) was used as a sensing element to measure gamma-ray spectra remotely with an LLG. $LaBr_3$:Ce, which is one of the most well-known commercialized lanthanide scintillators, has many advantages for gamma-ray spectroscopy, such as high density and effective Z-number, short decay time, and high light yield and sensitivity. However, owing to its hygroscopicity and short emission wavelength, $LaBr_3$:Ce cannot be used with typical optical fibers for remote sensing. LLG was originally invented to transmit UV light, and its core cross section is larger than that of a POF; it could be matched with a larger scintillator. The physical properties of $LaBr_3$:Ce are listed in Table 1 [14,15].

In this study, the LLG (Series 300, Lumatec) was used as a scintillation light deliverer. It transmits the light with total reflectance using all the available cross section and has excellent transmittance to the emission wavelength of the $LaBr_3$:Ce scintillator as shown in Fig. 1, which shows the light transmissivity of the LLG according to the wavelength [17]. The emission wavelength peak (360 nm) of $LaBr_3$:Ce is in the range from 320 to 440 nm, and the transmission of optical fiber is less than 40% in that wavelength range. In other words, the average transmission is less than 20% at peak wavelength and this means that only 20% of scintillation light from the $LaBr_3$:Ce can transmit through an optical fiber. Fig. 1 confirms that LLG has superior capability to transmit the scintillation light of $LaBr_3$:Ce compared to that of an optical fiber. Because of its open pipe cross section, unlike optical fiber bundles, it has no dead spots and can deliver light more efficiently. Moreover, due to its single polymer tube structure, it is very flexible and useful in rugged and narrow spaces. On the other hand, the commercially available LLGs have some weak points. The maximum diameter of an LLG is limited to about 10 mm due to the minimum bending radius and the high weight, and the operating temperature is also limited to −5 °C ~ +35 °C indefinitely, to −15 °C ~ +50 °C for a few days, and to −20 °C ~ +70 °C for a few hours due to bubble formation in the liquid filler. We used two different lengths of LLGs in this study: one with 8 mm core diameter and 1 m length and the other with the same core diameter and 3 m length.

Table 1
Physical properties of $LaBr_3$:Ce.

Properties	Value
Density (g/cm^3)	5.07
Effective Z-number	45.3
Decay time (ns)	15
Light yield (photons/MeV)	~66,000
Emission wavelength peak (nm)	360
Hygroscopicity	Yes

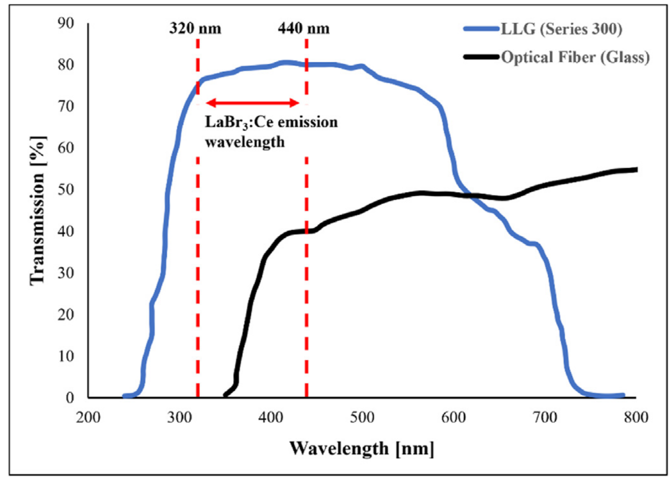

Fig. 1. Light transmissivities of the liquid light guide (LLG) and optical fiber.

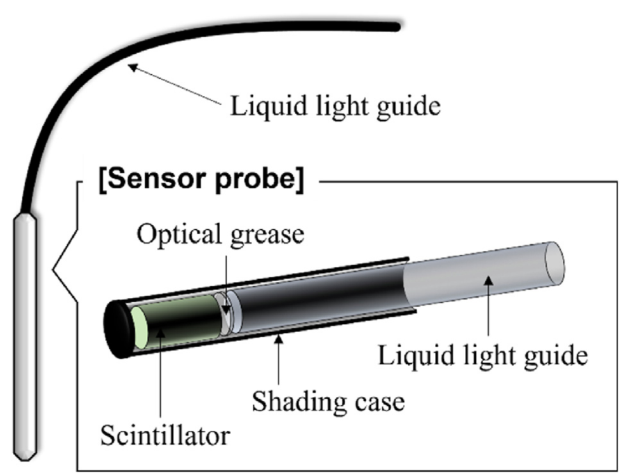

Fig. 2. Schematic diagram of the LLG radiation sensor.

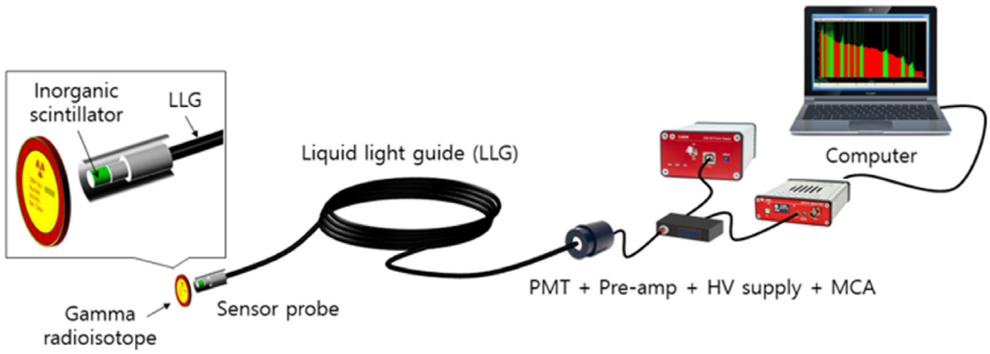

Fig. 3. Experimental setup for remote gamma-ray spectroscopy using the LLG radiation sensor.

Fig. 2 shows the schematic diagram of the proposed LLG radiation sensor. A cylindrical $LaBr_3$:Ce scintillator was sealed in an aluminum housing, and an optical grease (EJ-550, Eljen Technology) was applied to the interface between the housing window and the LLG for optimal light transmission by refractive index matching. The other end of the LLG was connected to a light-measuring device, and the optical grease was also applied to the interface between them. The dimensions of the scintillator were 8 mm diameter and 25 mm length, and the connection between the scintillator and the LLG was shaded by a black plastic case.

Fig. 3 shows the experimental setup for remote gamma-ray spectroscopy using the LLG radiation sensor. A photomultiplier tube (PMT, R6231-100, Hamamatsu) was used as a light-measuring device. The light generated from the scintillator was transmitted to the PMT through the LLG and converted into an amplified current signal. The converted signal was again amplified through a charge-sensitive preamplifier (Model 2007B, Mirion) and classified according to its amplitude by a multichannel analyzer (MCA). We used a digitizer (DT5725, Caen) that employed a Jordanov trapezoidal filter as the MCA.

For the experiment, Cs-137 and Co-60 gamma-ray sources were used. Their activities were 0.223 and 0.522 μCi respectively, and they were positioned on the scintillator without a gap during measurements. Every measurement was performed for 600 s.

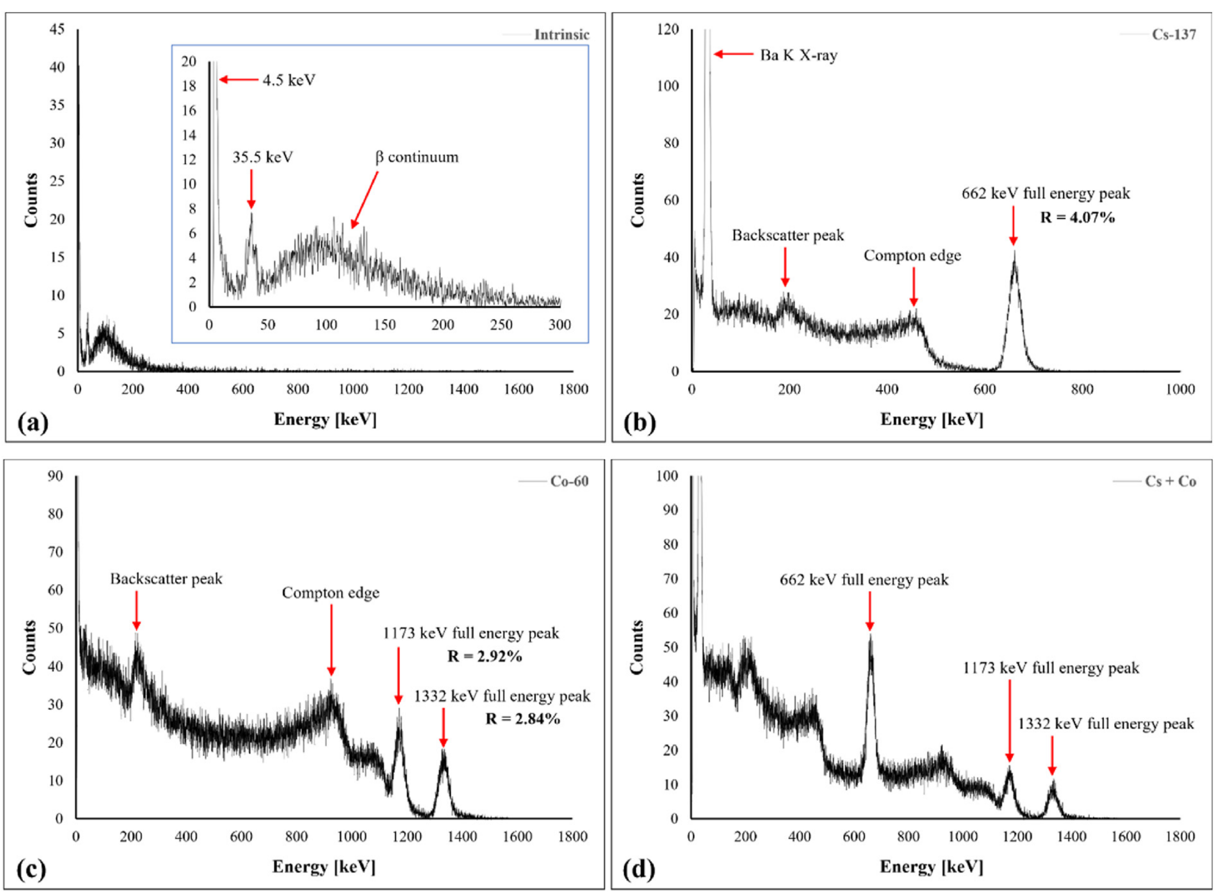

Fig. 4. Acquired energy spectra without the LLG for (a) intrinsic radioactivity of $LaBr_3$:Ce, (b) Cs-137, (c) Co-60, and (d) simultaneous measurement of Cs-137 and Co-60.

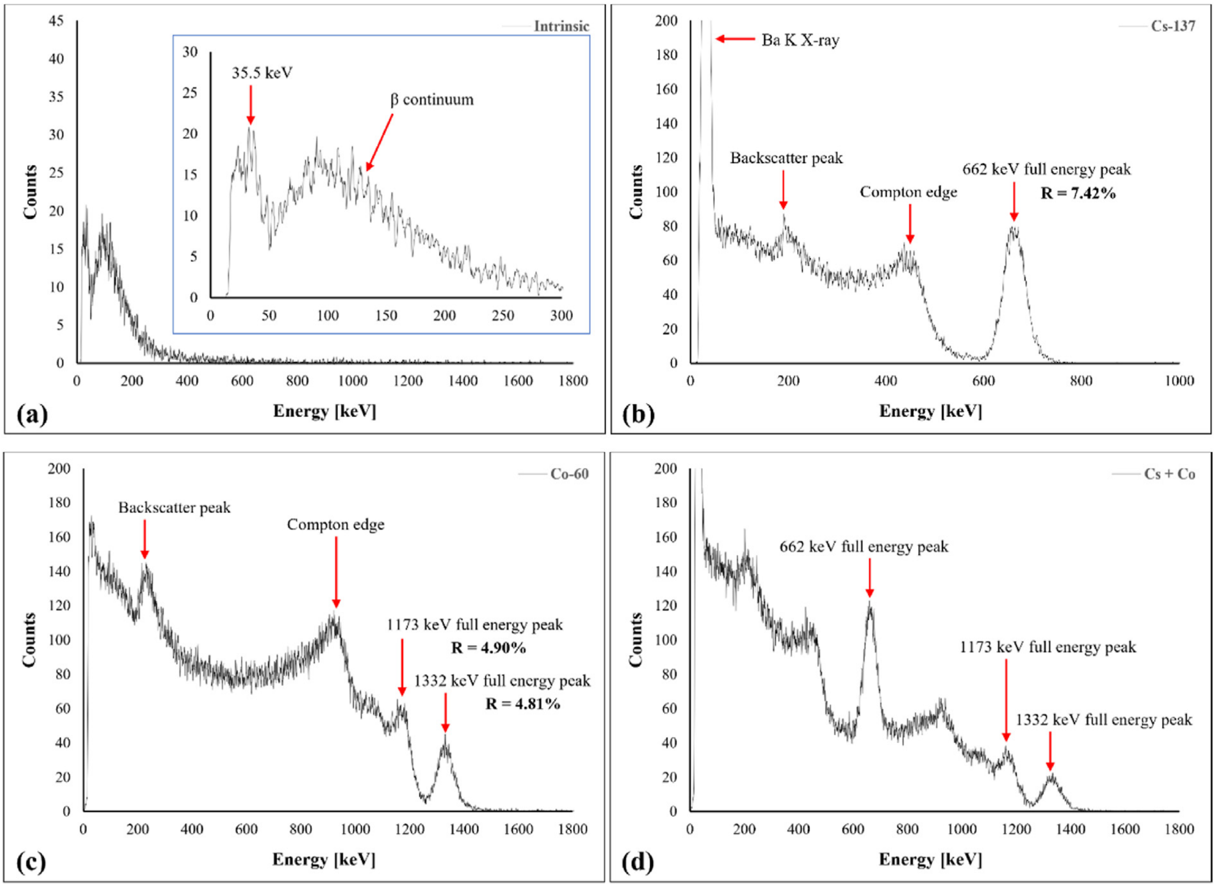

Fig. 5. Acquired energy spectra with an LLG length of 1 m for (a) intrinsic radioactivity of $LaBr_3$:Ce, (b) Cs-137, (c) Co-60, and (d) simultaneous measurement of Cs-137 and Co-60.

3. Experimental results

First, the gamma-ray spectra of Cs-137 and Co-60 were measured without the LLG. In this case, the scintillator was directly connected to the PMT through the optical grease. To avoid readout saturation, a bias voltage of +800 V was applied to the PMT. The trapezoidal rise time was optimized as 8 μs, which corresponded to 3 μs of shaping time for the traditional analog acquisition chain [18]. These set values were also maintained in the following measurements of gamma-ray spectra with the LLG.

Fig. 4 shows the results of gamma-ray spectroscopy without the LLG. Fig. 4(a) shows the background spectrum of $LaBr_3$:Ce in the absence of a gamma-ray source. This spectrum is caused by the intrinsic activity from the decay of La-138 in the scintillator. There are two main peaks at energies of 4.5 and 35.5 keV, which are observed in the spectrum. These peaks are induced by the electron captures in the decay of La-138; however, the 1436 keV gamma-ray from the decay is not observed because it escapes the scintillator [19]. This means that the size of the scintillator is insufficient for detecting gamma-rays from the decay of La-138, and the intrinsic activity of $LaBr_3$:Ce does not seriously affect the energy spectrum acquisition in this study. The continuum up to 255 keV is the β continuum due to the β-decay of La-138, and the induced 789 keV gamma-ray peak is not observed.

The acquired energy spectra of Cs-137 and Co-60 as well as their simultaneous measurement results are shown in Fig. 4(b) and (c), and 4(d), respectively. The full energy peaks of radionuclides are clearly observed in each result and the full-width-at-half-maximum (FWHM) values of each full energy peak were measured to calculate the energy resolution. The energy resolutions were estimated as 4.07%, 2.92%, and 2.84% at 662, 1173, and 1332 keV respectively.

The measured gamma-ray spectra of Cs-137 and Co-60 using the LLG radiation sensor are shown in Figs. 5 and 6. Fig. 5 shows the results with the LLG length of 1 m, and Fig. 6 shows the acquired spectra using the LLG sensor length of 3 m. As with the earlier results, all the major peaks were measured. From the 1 m LLG length results, the energy resolutions were 7.42% at 662 keV, 4.90% at 1173 keV, and 4.81% at 1332 keV, which were similar to the resolution of a general NaI(Tl) scintillation detector [15,20]. In the case of the 3 m LLG sensor, the energy resolutions were 7.92% at 662 keV, 5.48% at 1173 keV, and 5.07% at 1332 keV. The comparison with energy resolutions from other studies using a general NaI(Tl) scintillator is listed in Table 2.

According to the results, the energy resolution deteriorates upon using the LLG and increasing the length. In general, the energy resolution R of a scintillation detector is expressed as follows:

$$R = 2.35\sqrt{\frac{1+\upsilon(M)}{\overline{N}\overline{p}}} \tag{1}$$

where $\upsilon(M)$ is the variance in the PMT gain, $\overline{N}$ is the mean number of photons generated by the gamma-ray interaction with the scintillator, and $\overline{p}$ is the average transfer efficiency, which represents the probability of an electron produced at the first dynode of the PMT by a scintillating photon [21]. $\overline{N}\overline{p}$ eventually means the number of photoelectrons produced in the PMT [22,23].

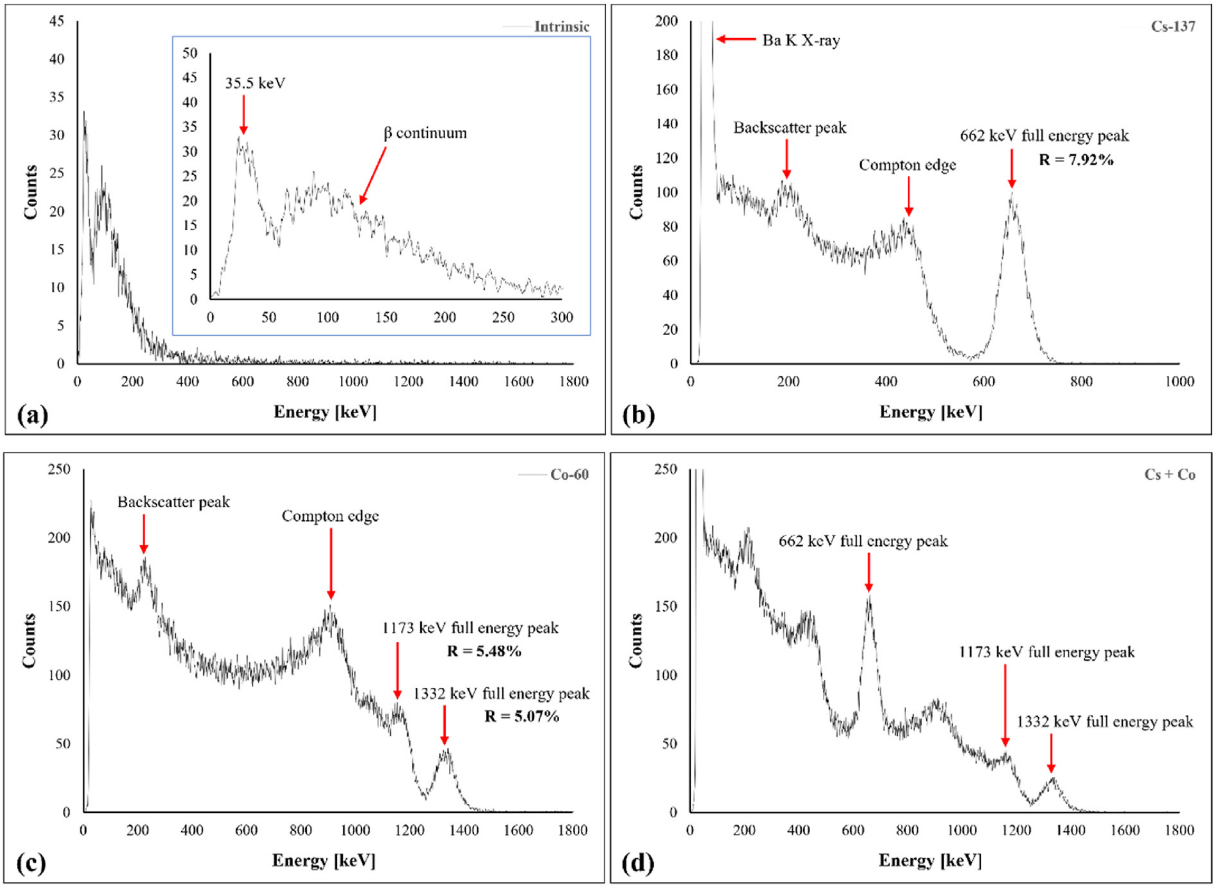

Fig. 6. Acquired energy spectra using the LLG length of 3 m for (a) intrinsic radioactivity of $LaBr_3$:Ce, (b) Cs-137, (c) Co-60, and (d) simultaneous measurement of Cs-137 and Co-60.

Table 2
Comparison with energy resolutions from NaI(Tl) scintillator.

Reference		Scintillator	Crystal dimension [mm^3]	Energy resolution at 662 keV
F.G.A. Quarati [15]		NaI(Tl)	Ø 51 × 51	7.2%
M. Balcerzyk [20]			Ø 25 × 31	6.7%
Our work	no LLG	$LaBr_3$:Ce	Ø 8 × 25	4.1%
	1 m LLG			7.4%
	3 m LLG			7.9%

The average transfer efficiency $\overline{p}$ depends on many factors, such as the wavelength of the scintillating photons, quantum efficiency of the PMT, transmissivity of the scintillating light through the crystal, reflectivity of the crystal covering, and optical coupling to the PMT window [21]. In this study, the loss of light by additional optical interfaces and the optical attenuation along the LLG would be the main factors. The additional optical interfaces may generate more reflections which cause the amount of guided light to be reduced. Eventually, because of the light attenuation through the LLG, $\overline{p}$ decreases and the number of photoelectrons produced at each event also decreases. Therefore, the denominator of Equation (1) decreases, and finally the energy resolution R increases.

Considering this statistical variation, the energy resolution R can be simply expressed as

$$R = \frac{K}{\sqrt{E}} \tag{2}$$

where E is the energy of the gamma-ray and K is a proportionality constant [24]. As shown in Fig. 7, linear relationships between the energy resolution and the square root of the gamma-ray energy are observed regardless of the LLG, and the gradient increases owing to the statistical variation according to the use of the LLG and the increase in its length.

The variation of $\overline{p}$ can also be confirmed in the analog-to-digital (ADC) channel of the uncalibrated energy spectrum. Fig. 8 shows the relationships between the ADC channel number and photopeak energy according to the length of the LLG.

The number of electrons collected at the PMT anode is expressed as

$$\overline{Q}_0 = \overline{N}\overline{p}\overline{M} \tag{3}$$

where $\overline{M}$ is the mean multiplication factor of the PMT [25,26]. The amplitude of the PMT output pulse varies with $\overline{Q}_0$, and the pulse is recorded at each ADC channel number according to its amplitude. Fig. 8 presents the relationship of the electrical signal amplitude measured by the MCA, which indicates how the energy information

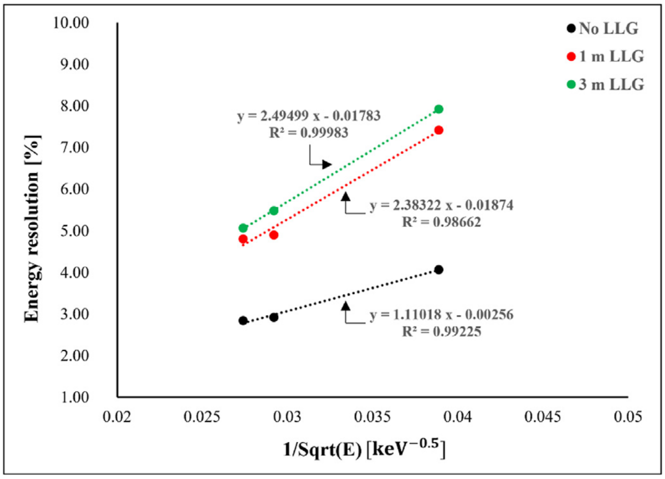

Fig. 7. Linear relationships between the energy resolution and the square root of the gamma-ray energy.

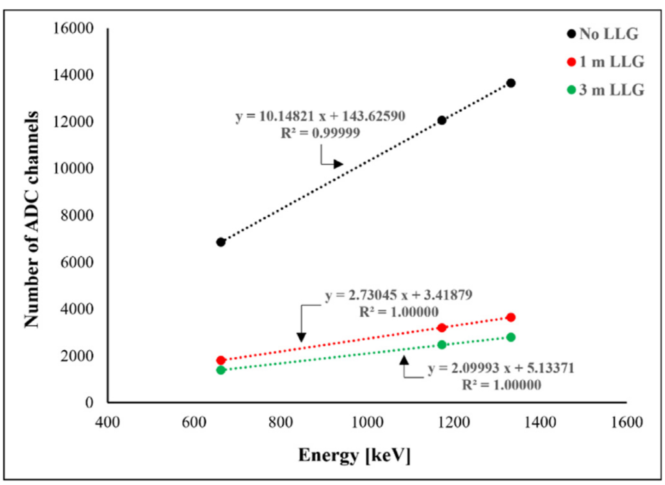

Fig. 8. Relationship between the ADC channel numbers and the photopeak energies according to the length of the LLG.

of the gamma-ray is expressed in the system. Good linearity is confirmed, where the amplitude of the electrical signal increases linearly as the energy of the incident gamma-ray increases, regardless of the use of LLG.

However, a drastic change is observed when the LLG is used. This drastic change is due to the loss of photons from $\overline{p}$ decrement, as in the previous case of energy resolution, which occurred because of the additional interfaces and path increment from the LLG employment. Otherwise, as shown in Fig. 8, the level of change according to the LLG length increment is not significant, and nuclide identification is possible through the energy spectra obtained with the LLG sensor. Given these results, the LLG radiation sensor is expected to be able to perform remote gamma-ray spectroscopy for distances of 3 m or more.

4. Conclusion

In this study, we fabricated a radiation sensor with a $LaBr_3$:Ce scintillator and an LLG and performed remote gamma-ray spectroscopy. We acquired the energy spectra of Cs-137 and Co-60, estimated the energy resolutions of the full energy peaks, and compared the scintillation light output variations.

The major peaks of the radionuclides were observed in each result. Energy resolutions were estimated as 7.42%, 4.90%, and 4.81% at 662, 1173, and 1332 keV, respectively, for a 1-m-long LLG, which were similar to the resolution of a general NaI(Tl) scintillation detector without an LLG. With a 3-m-long LLG, the energy resolutions were 7.92% at 662 keV, 5.48% at 1173 keV, and 5.07% at 1332 keV. In addition, we showed the relationships between energy resolution and ADC channel regarding the number of photoelectrons produced in the PMT and confirmed the effects of the length of an LLG on remote gamma-ray spectroscopy.

Considering the effects of photon loss, focusing the scintillation light at the center of the LLG is expected to be effective in improving energy resolution and reducing ADC channel decrement. Because randomly generated scintillation light within the scintillator enters the LLG at random angles, some photons carrying energy information of incident gamma-rays could travel a long spiral path or escape from the core of the LLG. These photons tend to attenuate strongly and eventually cause photon loss. To reduce these photons, the scintillation light should enter the light guide within its critical angle and its propagation path should be as close as possible to the central axis of the light guide. Lens focusing could be an efficient solution for this problem.

In further studies, the remote gamma-ray spectroscopy for longer distances will be performed using LLGs with more diverse lengths, and the mitigation of energy resolution deterioration by focusing scintillation light using lenses will be studied.

Declaration of competing interest

The authors declare that they have no known competing financial interests or personal relationships that could have appeared to influence the work reported in this paper.

Acknowledgements

This research was supported by the Korea Institute of Energy Technology Evaluation and Planning (KETEP) grant funded by the Korean government (MOTIE) (No. 20201520300060) and the National Research Foundation of Korea (NRF) grant funded by the Korean government (MSIT) (No. 2020M2D2A2062457, 2022M2D4A1084440).

References

[1] IAEA, Programmes and Systems for Source and Environmental Radiation Monitoring, Safety Reports Series No. 64, International Atomic Energy Agency, 2010.
[2] IAEA, Classification of Radioactive Waste, Safety Standards Series No. GSG-1, International Atomic Energy Agency, 2009.
[3] NRC, Consolidated Decommissioning Guidance: Characterization, Survey, and Determination of Radiological Criteria, NUREG-1757 2, U.S. Nuclear Regulatory Commission, 2006.
[4] DOE, Pipe Explorer Surveying System. Innovative Technology Summary Report, DOE/EM-0440, U.S. Department of Energy, 1999.
[5] M. Balaskó, E. Sváb, A. Kuba, Z. Kiss, L. Rodek, A. Nagy, Pipe corrosion and deposit study using neutron- and gamma- radiation sources, Nucl. Instrum. Methods Phys. Res. 542 (2005) 302–308, https://doi.org/10.1016/j.nima.2005.01.153.
[6] K.-T. Han, W.J. Yoo, J.K. Seo, S.H. Shin, D. Jeon, S. Hong, S. Cho, J.H. Moon, B. Lee, Optical fiber-based gamma-ray spectroscopy with cerium-doped lutetium yttrium orthosilicate crystal, Opt. Rev. 20 (2013) 205–208, https://doi.org/10.1007/s10043-013-0036-z.
[7] W.J. Yoo, S.H. Shin, D.E. Lee, K.W. Jang, S. Cho, B. Lee, Development of a small-sized, flexible, and insertable fiber-optic radiation sensor for gamma-ray spectroscopy, Sensors 15 (2015) 21265–21279, https://doi.org/10.3390/s150921265.
[8] Y.B. Song, S.H. Shin, S.W. Song, H.J. Kim, S. Cho, B. Lee, Feasibility study on remote gamma spectroscopy system with fiber-optic radiation sensor, J. Radioanal. Nucl. Chem. 316 (2018) 1301–1306, https://doi.org/10.1007/s10967-018-5754-z.
[9] B. Lee, K.W. Jang, D.H. Cho, W.J. Yoo, G.-R. Tack, S.-C. Chung, S. Kim, H. Cho,

Measurements and elimination of Cherenkov light in fiber-optic scintillating detector for electron beam therapy dosimetry, Nucl. Instrum. Methods Phys. Res. 579 (2007) 344–348, https://doi.org/10.1016/j.nima.2007.04.074.
[10] K. Nomura, A. Yunoki, M. Hara, Y. Morito, A. Fujishima, Development of a flexible γ-ray detector using a liquid scintillation light guide (LSLG), Appl. Radiat. Isot. 139 (2018) 12–19, https://doi.org/10.1016/j.apradiso.2018.04.018.
[11] M. Hayashi, J. Kawarabayashi, K. Asai, H. Iwai, Y. Nakagawa, T. Iguchi, Position-sensitive radiation detector with flexible light guide and liquid organic scintillator to monitor distributions of radioactive isotopes, J. Nucl. Sci. Technol. 45 (2008) 81–84, https://doi.org/10.1080/00223131.2008.10875982.
[12] J. Kawarabayashi, R. Mizuno, D. Inui, K. Watanabe, T. Iguchi, Potential on liquid light guide as distributed radiation sensor, IEEE Symposium Conference Record Nuclear Science 2 (2004) (2004) 712–714, https://doi.org/10.1109/NSSMIC.2004.1462310.
[13] E.V.D. van Loef, P. Dorenbos, C.W.E. van Eijk, High-energy-resolution scintillator: Ce3+ activated LaBr3, Appl. Phys. Lett. 79 (2001) 1573–1575, https://doi.org/10.1063/1.1385342.
[14] F. Quarati, A.J.J. Bos, S. Brandenburg, C. Dathy, P. Dorenbos, S. Kraft, R.W. Ostendorf, V. Ouspenski, A. Owens, X-ray and gamma-ray response of a 2"×2" LaBr3:Ce scintillation detector, Nucl. Instrum. Methods Phys. Res. 574 (2007) 115–120, https://doi.org/10.1016/j.nima.2007.01.161.
[15] F.G.A. Quarati, P. Dorenbos, J. van der Biezen, A. Owens, M. Selle, L. Parthier, P. Schotanus, Scintillation and detection characteristics of high-sensitivity CeBr3 gamma-ray spectrometers, Nucl. Instrum. Methods Phys. Res. 729 (2013) 596–604, https://doi.org/10.1016/j.nima.2013.08.005.
[16] B. Löher, D. Savran, E. Fiori, M. Miklavec, N. Pietralla, M. Vencelj, High count rate γ-ray spectroscopy with LaBr3:Ce scintillation detectors, Nucl. Instrum. Methods Phys. Res. 686 (2012) 1–6, https://doi.org/10.1016/j.nima.2012.05.051.
[17] Lumatec, Liquid light guide datasheet. Available online: https://lumatec.de/files/5415/0643/4704/brochure-liquid-light-guide-en.pdf.
[18] Caen, MC2Analyzer User manual. Available online: https://www.caen.it/support-services/documentation-area/?documentbyname=mc2analyzer&type=all-categories.
[19] F.G.A. Quarati, I.V. Khodyuk, C.W.E. van Eijk, P. Quarati, P. Dorenbos, Study of 138La radioactive decays using LaBr3 scintillators, Nucl. Instrum. Methods Phys. Res. 683 (2012) 46–52, https://doi.org/10.1016/j.nima.2012.04.066.
[20] M. Balcerzyk, M. Moszyński, M. Kapusta, Comparison of LaCl3:Ce and NaI(Tl) scintillators in γ-ray spectrometry, Nucl. Instrum. Methods Phys. Res. 537 (2005) 50–56, https://doi.org/10.1016/j.nima.2004.07.233.
[21] P. Dorenbos, J.T.M. de Haas, C.W.E. van Eijk, Non-proportionality in the scintillation response and the energy resolution obtainable with scintillation crystals, IEEE Trans. Nucl. Sci. 42 (1995) 2190–2202, https://doi.org/10.1109/23.489415.
[22] P. Dorenbos, Light output and energy resolution of Ce3+-doped scintillators, Nucl. Instrum. Methods Phys. Res. 486 (2002) 208–213, https://doi.org/10.1016/S0168-9002(02)00704-0.
[23] I.V. Khodyuk, P. Dorenbos, Nonproportional response of LaBr3:Ce and LaCl3:Ce scintillators to synchrotron x-ray irradiation, J. Phys. Condens. Matter 22 (2010) 485402–485408, https://doi.org/10.1088/0953-8984/22/48/485402.
[24] G.F. Knoll, Radiation Detection and Measurement, third ed., John Wiley & Sons, Inc., New York, 2000.
[25] C. Kuntner, E. Auffray, P. Lecoq, C. Pizzolotto, M. Schneegans, Crystal Clear Collaboration, Intrinsic energy resolution and light output of the Lu0.7Y0.3AP:Ce scintillator, Nucl. Instrum. Methods Phys. Res. 493 (2002) 131–136, https://doi.org/10.1016/S0168-9002(02)01559-0.
[26] J.B. Birks, The Theory and Practice of Scintillation Counting, first ed., Pergamon, New York, 1967.